DEVELOPMENT OF HYBRID WIND TURBINE GENERATOR AND SOLAR POWER SYSTEM MODEL FOR RURAL ELECTRIFICATION

OSHIN, Ola Austin
Department of Electrical Electronics Engineering
Elizade University, Ilara-Mokin, Ondo State

ABSTRACT
The countries that are most energy-consuming, where there are industrial developments, where the energy demand is highest are the advanced and developing countries in the world (Mustafa, 2018). For instance, the average power per capital (watts per person) in the United States is 1,377 Watts. In Canada, it is as high as 1,704 Watts per person and in South Africa; it is 445 Watts per person. The average power per capital in Australia is 1,112 Watts and in New Zealand it is 1,020 W per person. Whereas, the average power per capital (watts per person) in Nigeria is 14 W per person. (Austin, O. O et.al, 2020). Also, power supply in many parts of Africa is erratic and characterized with a lot of faults and outages. In Nigeria, it is estimated that only 40 % of Nigerians are connected to the national grid and the connected population are exposed to frequent power outages (Abubakar *et al*, 2015, Austin O.A, 2020). Unfortunately, the effects of incessant power supply have destroyed many industrial activities, reduced employment and has increased crime activities in many parts of the continent (Africa). Therefore, in order to provide urgent solution to these problems and satisfy the high energy demand in African residential and industrial environments, electrical energy should be reliable, affordable, effective, and sustainable. This calls for an urgent establishment of alternative Renewable Hybrid Power Supply System which will provide continuous, reliable and effective power supply to the consumers. Hence, in this research work, feasibility assessment of the study area for the establishment of Hybrid Power System (HPS) was carried out. The operating parameters and performances of the components of the Hybrid Power System were evaluated and the HPS Simulink models were developed using MATLAB/Simulink 8.1064 (2020a) version software. The Hybrid Power System Model (HPSM) developed comprises of Solar Photo Voltaic System (SPVS) and Wind Turbine Generator (WTG) Models. Simulation of the developed Simulink models were carried out. Optimization process was carried out using Optimum Power Point Tracking (OPPT) Techniques and Genetic Algorithms (G.A). Design processes and control algorithms were established for the production of reliable and efficient output power from the Hybrid Power System. Simulink and validation results obtained made it possible to generate and supply continuous, reliable, effective and stable electrical power to the consumers. Finally, the developed HPS model in this research work was found to be very useful for the establishment of Hybrid Power Plants which guarantees the supply of continuous, stable and reliable electric power for various residential and industrial consumers.

INTRODUCTION TO HYBRID RENEWABLE ENERGY SYSTEM

The demand for electricity which is increasing on daily basis cannot be fulfilled by non-renewable energy sources alone. Hence, there is a great need for harnessing the energy supplied by renewable energy resources. Hybrid renewable energy sources are emerging alternatives to provide solution to the incessant power supply and insufficient energy provided by the non-renewable energy sources. It is the composition of two or more renewable energy resources that work in stand-alone or grid connected mode. It can also be referred to the composition of two or more renewable energy resources with or without conventional energy sources. (Vikas Khare et.al, 2016).

The combined utilization of these renewable energy sources is called Hybrid Renewable Energy Systems or Hybrid Electric Power System (HEPS). For optimum performance, two or more forms of energy resources are combined to form a hybrid energy system. This complements the drawbacks in each individual energy resources. (Ibrahim Baba Kyari, et. al, 2019).

AIM

The aim of the research is to develop a wind and solar Hybrid Power System Model for the operation and design of renewable energy system and develop an effective Hybrid Power System model with Optimum Performance using Optimum Power Point Tracking (OPPT) Techniques.

OBJECTIVES

1. To evaluate the operating parameters and performances of the components of the Hybrid Power System Model (HPSM)
2. To develop Simulink models of the HPSM using MATLAB/Simulink 8.1.0604 (2020a) version software.
3. To develop an effective Hybrid Power System model with Optimum Performance using Optimum Power Point Tracking (OPPT) Techniques.

LITERATURE REVIEW

Operating Performances of the Solar Photovoltaic System (SPVS)

A PV module or array is made up of a number of solar cells which are connected in series and parallel as shown in figure 2.1. When solar light radiation falls on PV cells, light energy is converted to electrical energy without any moving parts. The transmitted light is absorbed within the semiconductor, and electrical energy is generated by using this light energy to excite free electrons

from the low energy status to an unoccupied higher energy level. As a result, electron-hole pair combinations will take place in the p-n junction semiconductor diode causing the flow of electrical current. The IV and PV characteristics of the solar PV module varies with different temperature and irradiance conditions. (Meenal Jain, Nilanshu Ramteke ,2013; Elias M.Salilih and Yilma T.Birhane, 2019)
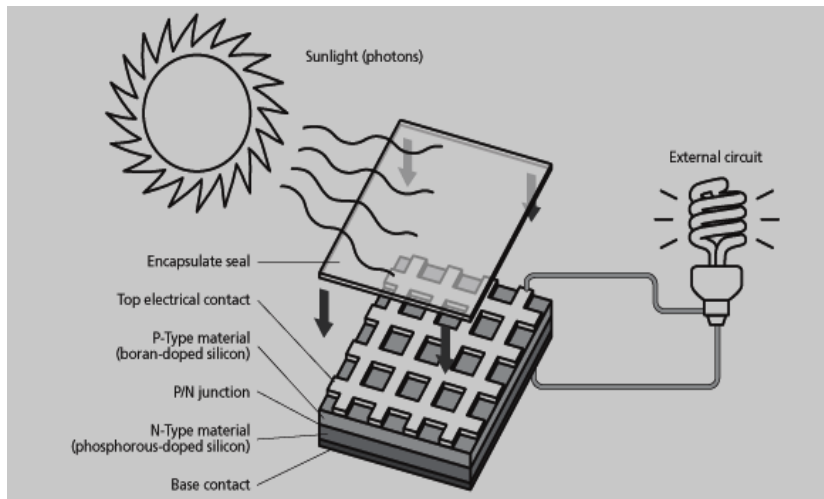
Fig, 2.1: Conversion of light energy to electrical energy in a Solar PV module

SINGLE DIODE MODEL WITH SHUNT RESISTANCE

The solar PV circuit model shown in figure 2.2 contains the current source I_{ph} which depends on cell temperature and solar radiation, a diode in which the reverse saturation current (I_D) depends mainly on the operating temperature, a series resistance (R_s). and a shunt resistance (R_{sh} or R_p) which takes into account the losses in PV cell. (Meenal Jain, Nilanshu Ramteke, 2013, Julius Simiyu e.tal 2019)
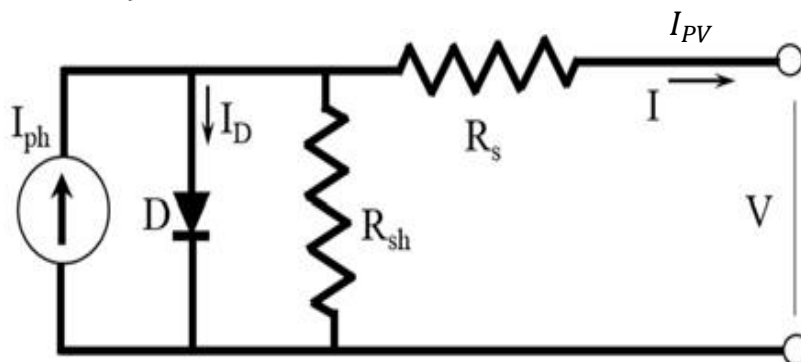

Figure 2.2: A single diode model with shunt resistance

Model equations of the output current of the solar photovoltaic is presented in equations 2.1 – 2.4

$$I_{PV} = N_P I_{ph} - N_P I_S \left[\exp \frac{\left(\frac{V}{N_S} + \frac{I R_S}{N_p} \right)}{AKT} - 1 \right] - \left[\frac{\frac{V * N_P}{N_S} + I R_S}{R_{sh}} \right] \qquad \textbf{2.1}$$

Where

i. N_P = number of parallel cells
ii. N_S = number of series cells
iii. I_{PV} = *output current*, I_D = Diode current
iv. I_{ph} = light generated photo current
v. I_{rs} = cell reverse saturation current at T_{ref}
vi. I_{SC} = Short circuit current at reference temperature 25° C
vii. I_S = Cell saturation current current at T_{ref}
viii. T_{nom} = T_{ref} = reference temperature in celsius

ix. The reference values will be taken from the PV module manufacturers datasheet for specified operating condition such as STC (standard test conditions) in which the irradiance is 1000W/m²
x. K_i = Short circuit current temperature coefficient at I_{SCR}
xi. K = Boltzmann's constant 1.38 * 10⁻²³ J/K
xii. T = Cell temperature in Celsius
xiii. q = Charge of electron = 1.6×10^{-19} C
xiv. λ = Solar irradiation in Watts/m²
xv E_g = Band gap energy for silicon and A = Ideality factor
xvi. T_{nom} = T_{ref} = Reference temperature in Celsius = 25 degree celsius
xvii. I_S = Cell saturation current at T_{nom}
xviii. R_{sh} = Shunt resistance in ohms
xix. R_s = Series resistance in oh

a. The reverse saturation current (Irs) gis given in equation

$$I_{rs} = I_{SC} \ / \ \left[.\exp \ \frac{(q*V_{oc})}{N_S AKT} - 1 \right] \qquad 2.2$$

When a diode is reverse biased, the depletion region width increases and majority carriers move away from the junction such that there is no flow of current due to majority carriers. However, there are thermally produced minority electron hole pair combinations which are forward biased during reverse bias condition. These minority carriers will cause current to flow in the circuit. This current is usually very small (within the range of micro amp to nano amp). Since this current flow is due to minority carriers at a given temperature, the current is known as **reverse saturation current**

The saturation current (Is) is given in equation

$$I_S = I_{rs} \left[\frac{T}{T_r} \right]^3 \left[\exp \left(E_{g*} \ \frac{q \ (T - T_r)}{A* \ K.T.T_r} \right) \right] \qquad 2.3$$

Observation revealed that the photocurrent I_{ph} varies with cell short circuit current I_{SCR}, cell temperature T, cell referred temperature T_r, short circuit current temperature coefficient k_1 and solar radiation S (in mW/cm^3) as shown in the equation 2.4:

$$I_{ph} = \left[I_{SCR} + k_1 \ [T - T_r] \right] \frac{S}{100} \qquad 2.4$$

The Practical Single Diode PV Cell Model
Figure 2.3 shows a practical single PV cell model with the mathematical model equations shown in equations 2.5 − 2.7

$$1 = I_{ph} - I_D - I_{sh} \qquad 2.5$$

1 = cell current, I_{ph} = photo current, I_D = diode current, A = diode constant, q = charge of the electron, K = Boltzmaan's constant, I_0 = cell saturation current, V = cell voltage,
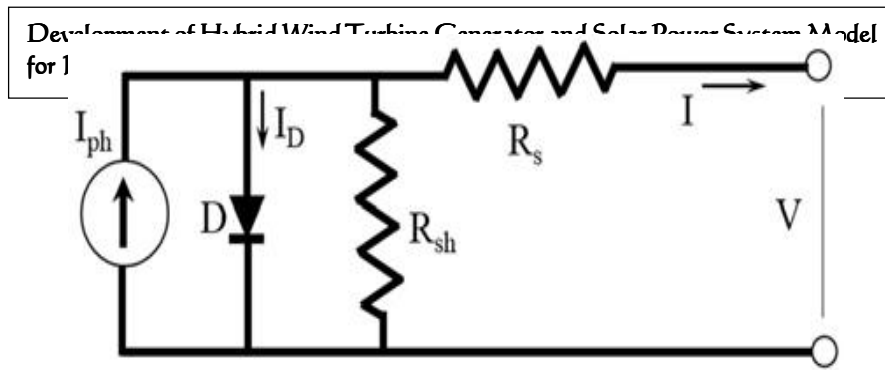
Figure 2.3: Practical single PV cell model

T = cell temperature (K), R_s = series resistance and R_{sh} = shunt resistance

Diode current $I_D = I_0 \left[.\exp\left(\frac{q\,(V + I\,R_s)}{AKT} - 1\right) - \frac{(V + I\,R_s)}{R_{sh}} \right]$ 2.6

Therefore, $I = I_{ph} - I_D$ will become

$I = I_{ph} - I_0 \left[.\exp\left(\frac{q\,(V + I\,R_s)}{AKT} - 1\right) - \frac{(V + I\,R_s)}{R_{sh}} \right]$ 2.7

MAXIMUM POWER POINT TECHNIQUES (MPPT) IN A WTG USING TIP SPEED RATIO (TSR) CONTROL TECHNIQUES

Power generated in the wind turbine generator can be controlled by the Tip Speed Ratio (TSR) control techniques. This is done by keeping the Tip Speed Ratio in its optimal value in a variable speed generation. Hence, the aim of this method of Maximum Power Point Techniques (MPPT) process is to determine the optimum TSR by measuring the wind speed and rotor speed using the mathematical model equation below.

The Tip Speed Ratio $= \frac{R\omega}{V}$

Where   R = Radius of the turbine (m)

ω = angular speed of the tip of a blade in rad/sec

V = average wind speed in m/s

i. The optimum tip speed ratio λ_{opt} is attained when the coefficient of performance C_p of the WTG is maximum as shown in the figure 2.28. For Wind Turbine generator, coefficient of performance C_p is less or equal to 0.593

ii. The maximum rotor speed of the wind Turbine generator can then be obtained

Optimum rotor speed $= \omega_{optimum} = \frac{\lambda_{optimum}}{R} V_{windspeed}$ 2.8

Hence, the maximum Power Point is obtained when the rotor is running at optimum rotor speed $(\omega_{optimum})$.

Maximum Power Point is obtained when the turbine shaft (ω_r) is optimum as shown in figure 2.4
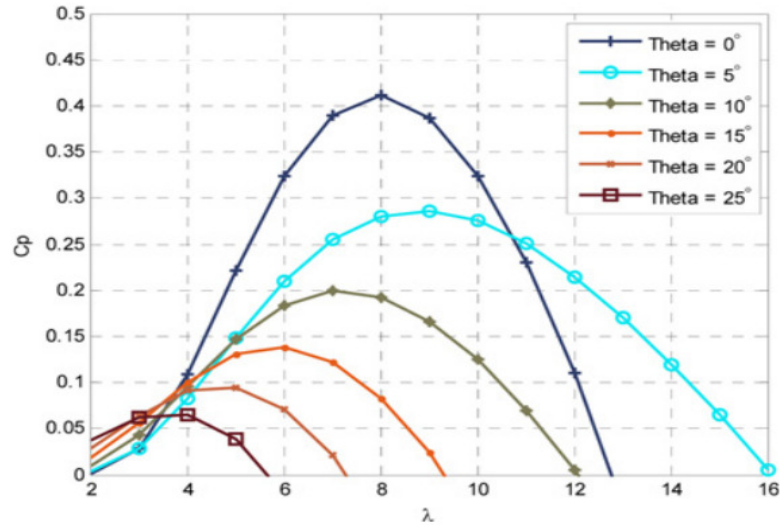

Figure 2.4: showing the coefficient of performance, C_p, and the Tip Speed Ratio λ
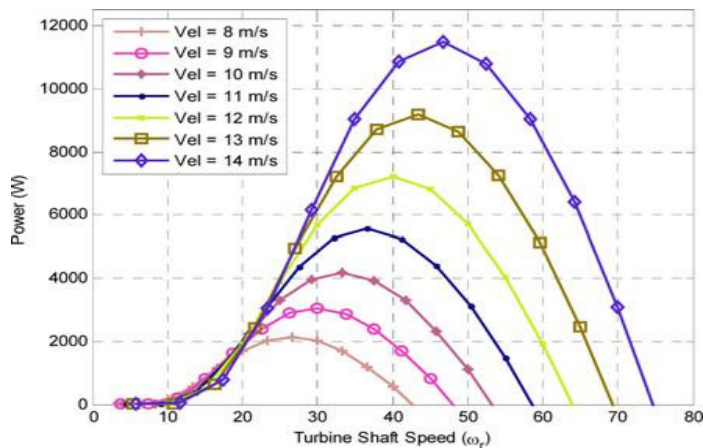

Figure 2.5: Wind Turbine Power Curve

If the angular speed is higher than the reference or desired turbine shaft speed at which maximum power can be obtained, then, the angular speed should be reduced in order to obtain the maximum output power. If the angular speed is lower than the turbine shaft speed at which maximum power can be obtained, then, the angular speed should be increased This process of changing the

angular speed of the turbine in order to obtain maximum output power is called Maximum Power Point Tracking.

Maximum Power Point Tracking Techniques

Solar and wind require special control system unlike diesel power plant or generator in which output power is controlled by varying the speed of the rotor, changing the magnetic field around the stator and the rotor and controlling the inflow of fuel. Maximum Power Point can be obtained in a Wind Turbine Generator (WTG) by using Perturb and Observe (P & O) or Hill Climb Searching (HCS) iteration method, Optimum Torque Control (OTC) and Optimum Tip Speed Ratio Control (OTSR). The amount of electrical energy generated in a wind turbine generator depends on rotational speed of the rotor. The rotational speed should be varied in order to obtain optimum Tip Speed Ratio (TSR) shown in figures 2.4 and 2.5.

The Tip Speed Ratio was obtained from the ratio of the rotational speed of the tip of a blade to the wind speed, V in a given direction.
Measurement of the speed of the blade was done by using tachometer. The wind speed was measured by using anemometer. The value of the TSR obtained was compared with the optimum value of the TSR which has been stated on the generator. This was done continuously and the difference was fed back into the controller which adjusted the speed of the WTG to operate at or close to the optimum value of the TSR. Maintaining optimum TSR leads to the generation of electric power in a Wind Turbine Generator at maximum point and efficiency.

Maximum Power Point Tracking Techniques in Solar Photo-Voltaic System

In a photo-voltaic System, maximum power point can be obtained by varying solar insolation. This can be done by using stepper motor control system, Perturb and Observe (P & O) or Hill Climb Searching (HCS) iteration method, Open Circuit Based MPPT Techniques (OCBT), Incremental Conductance Method (ICM), Look Up Table and Curve Fitting Method (LTCFM), and Parasitic Capacitance Algorithm (PCA). With these MPPT tracking techniques, installation cost will reduce, efficiency will increase, and the performance and efficiency of the hybrid system will increase.

Perturb and Observe Method (P & O)

P&O is the most often and widely used method because of its simple feedback structure and fewer measured parameters. P&O for solar system involves periodically increase or decrease of solar output voltage and look for the corresponding power change. If a given perturbation leads to an increase in the array power then the subsequent perturbation is done in the same direction otherwise perturbation is done in opposite direction. Maximum power is obtained when the derivative of variation of output power to voltage shown in figure 2.6 is zero.
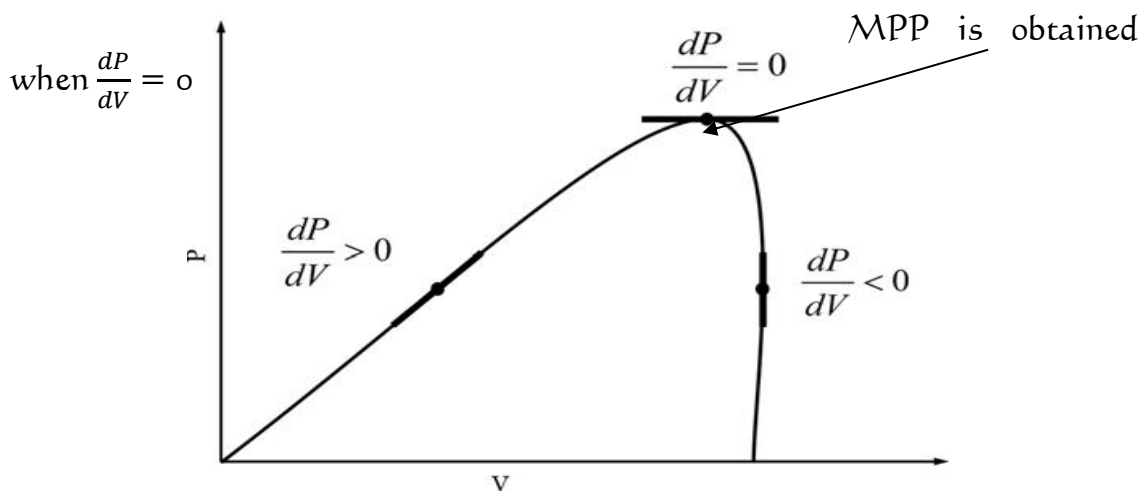

Fig. 2.6: Maximum Power Point Tracking in Solar Photo-Voltaic System

Modelled Wind Power System

The model equation for wind power system is shown in equation 2.9:

$$P_{wind} = \frac{1}{2} \, C_p \, \lambda \rho \, A \, V^3 \qquad\qquad 2.9$$

Where
- (P) = Power Output of the wind turbine in kilowatts
- (ρ) = Air Density, measured in kilogram per cubic meter
- (A) = intercepting area of the rotor blade in square meter
- (V) = Wind Speed, miles/seconds
- λ = Tip Speed Ratio (TSR)

(Cp) = Turbine power efficiency coefficient or coefficient of performance, Bertz coefficient which is a maximum of 0.593

METHODOLOGY

This research work developed a Hybrid Power System Model for feasibility assessment and establishment of renewable energy. It provides reliable, efficient and low-cost electric power from Hybrid Electric Power System (HEPS) model shown in figure 3.1.
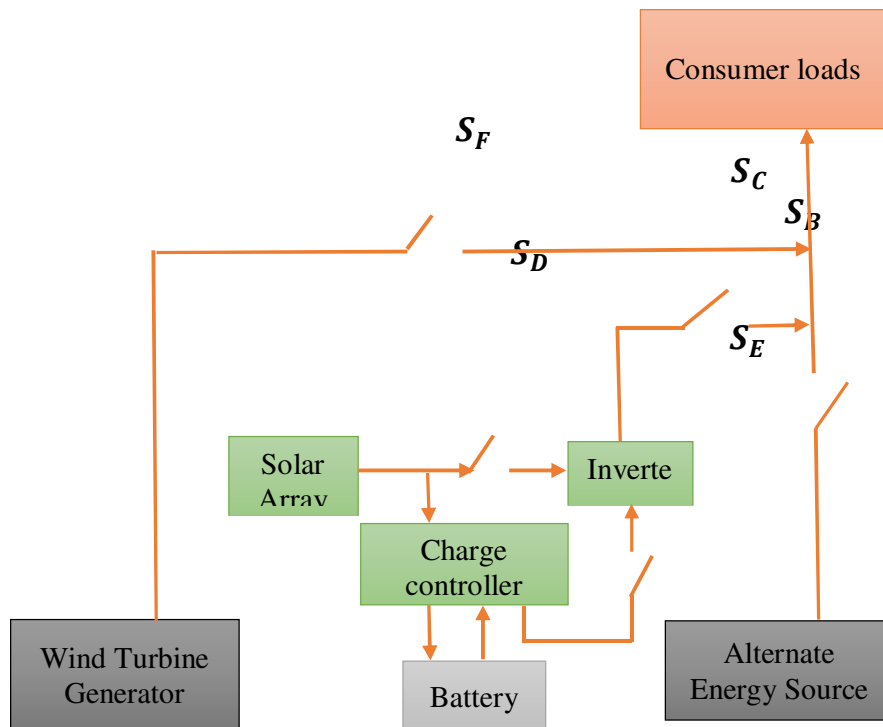
Figure 3.1: Hybrid Electric Power System (HEPS)

Figure 3.1: Hybrid Electric Power System (HEPS)

Energy Consumption and Meteorological Data Analysis

Energy audit data and Meteorological data were collected from Kwara State University with energy consumption in watt hour given as 1,865,500 Watt hour

This implies that the total energy to be supplied = 1,865,500 Wh

$$\text{Watt peak} = \frac{\text{Energy to be supplied}}{\text{number of hours of sunlight}} = \frac{1,865,500 \text{ Wh}}{7} = 266,500$$

$$\text{Number of 325 W panels} = \frac{\text{Watt peak}}{\text{Wattage of a solar panel}} = \frac{266,500}{325} = 820$$

System voltage = Voltage of a battery x number of batteries in series = 12 X 82 = 924 V

Charge to be stored in the solar system $= \dfrac{Grand\ total\ energy\ x\ Day(s)\ of\ autonomy}{nomoinal\ Voltage}$ **3.1**

Charge to be stored in the solar system $= \dfrac{1,865,500\ x\ 1}{12} = 155,485.33$ Ampere hour (Ah)

System Current $= \dfrac{Total\ power}{system\ voltage} = \dfrac{245,073.4}{924} = 265.231$ A

Land Area $=$ Area of one module x number of modules $= 1.63 \times 820 = 1,328.4 m^2$

200 Ah batteries were used at the reference area.

Hence,

Number of batteries required $= \dfrac{Charge\ to\ be\ stored\ in\ the\ solar\ system}{0.85\ x\ rating\ of\ a\ battery\ in\ Ah\ x\ depth\ of\ discharge}$ **3.2**

The depth of discharge is 70% while 0.85 accounts for battery loss

Hence, number of batteries required $= \dfrac{155,485.33}{0.85\ x\ 200\ x\ 0.7} = 1306.599$, approximately equal to 1,307

1. Latitude (ψ) and longitude of the location are $8^0\ N$, $5^0\ E$ respectively
2. Average solar insolation: 278–330 days of sun per year with daily average sunshine ranging from 6 hours during the rainy season to 9 hours in dry season
3. Solar radiation is the incident energy per unit area on a surface. Solar irradiance (SI) is the power per unit area (watt per square metre, W/m^2) received from the Sun in the form of electromagnetic radiation Maximum power is generated when the tilt angle is equal to the latitude of the location.
4. The monthly average clear sky daily global irradiance (H_C) for the location in Wh/m^2/day can be estimated using equation 3.9.

$$H_C = \frac{24\ X\ I_{sc}}{\pi}\left[1 + 0.033\cos\left(\frac{360n}{365}\right)\right]x\cos\emptyset\cos\delta\sin w_s + \left(\frac{2\pi w_s}{360}\right)\sin\emptyset\sin\delta \quad \textbf{3.3}$$

$I_{sc} =$ solar constant $= 1000\ W/m^2$

n $=$ average daylight length

N $=$ maximum possible sunshine duration

H $=$ monthly average daily global radiation in Wh/m^2/day

$H_C =$ monthly average clear sky daily global radiation for the location in Wh/m^2/day

a and b are empirical constants

$E_o =$ eccentricity correction $= 1 + 0.033\cos\left(\frac{360nd}{365}\right)$

Where nd is the number of days in the year starting 1st of January to December

$31^{st} = 365$, E_o = eccentricity correction = $1 + 0.033 \cos\left(\frac{360nd}{365}\right)$ 3.4

$$= 1 + 0.033 \cos 360 = 1.33$$

5. The angle measured from the centre of the sun to the centre of the earth is known as angle of declination δ. This value was obtained using equation 3.5

$$\delta = 23.45 \sin\left[360\left(\frac{284 + n}{365}\right)\right]$$ 3.5

$$= 23.45 \sin\left[360\left(\frac{284 + 365}{365}\right)\right] = 23.45 \sin\left[360\left(\frac{649}{365}\right)\right]$$

$$= 23.45 \sin[640.11] = 23.086$$

Latitude of the location = $\psi = 8^0\,24' = 8.4^0$, daily average value of sun shine length $N = \frac{2}{15}W_s$

Where W_s = mean sunset hour angle, N = daily average value of sun shine length and n = number of hours in a day

$$a = -0.11 + 0.235 \cos\psi + 0.323\frac{n}{N}$$ 3.6

$$= -0.11 + 0.235 \cos 8.4 + 0.323\frac{24}{7} = -0.11 + 0.2323 + 1.1074 = 1.2297$$

$$b = 1.45 + 0.553 - 0.694\frac{n}{N}$$ 3.7

$$= 1.45 + 0.553 - 0.694\frac{24}{7} = -0.3764$$

Where, clearness index, $K_t = \frac{H}{H_o} = a + b\left[\frac{n}{N}\right]$ 3.8

$$\frac{H}{H_o} = 1.2297 + -0.3764\left[\frac{24}{7}\right] = -0.0606$$

Defined as the surface radiation divided by the extraterrestrial radiation. It represents the fraction of the solar radiation that is transmitted through the atmosphere to strike the surface of the earth.

RESULTS OF THE OUTPUT CURRENT OF THE PHOTOVOLTAIC CELL

The output current of the Photovoltaic cell, I, under varying irradiance and temperature were obtained using equations 4.1 – 4.3 and the results were simulated using Matlab Simulink Software.

$$I = I_{ph} - I_s\left[\exp\left(\frac{qV_{oc}}{AkT_c}\right) - 1\right]$$ 4.1

$$I_{ph} = \left[I_{sc} + K_i\left(T_C - T_{ref}\right)\right]$$ 4.2

$$I_S = I_{RS} \left[\frac{T_c}{T_{ref}}\right]^3 \exp\left[\frac{q\,E_G\,\left(\frac{1}{T_{ref}} - \frac{1}{T_c}\right)}{KA}\right] \qquad 4.3$$

I = output current of the Photovoltaic cell

I_{ph} = photo current

I_s = saturation current

q= elementary charge = (1.6022×10^{-19}) C

V_{oc} = open circuit voltage of a module = 3.1 V

A = Ideality factor (IF) = 1.13

K=Boltzmann's constant = $1.38 \ x \ 10^{-23}$ J/K

T_c = temperature of the location

I_{sc} = short circuit current at reference temperature of 25^0 C and solar radiance of 1000 W/m^2 = 13.1362 A

K_i = short circuit current temperature coefficient = - 0.03

Photo current at 40^0 C was obtained using equation 4.1

$$I_{ph} = \left[I_{sc} + K_i\left(T_C - T_{ref}\right)\right] \times \boldsymbol{\lambda}$$
$$I_{ph} = [13.1362 + -0.03\,(40 - 25)] \times 1$$
$$I_{ph} = [3.1362 + -0.45\,] = 12.6862 \text{ A}$$

THE REVERSE SATURATION CURRENT (IRS) OF THE PHOTOVOLTAIC CELL

The reverse saturation current (Irs) at reference temperature and at varying temperature were obtained and the results were simulated using Matlab Simulink Software.

$$I_{rs} = I_{SC} / \left[. \exp \frac{(q * V_{oc})}{N_S AKT}\right] - 1$$

$$I_{rs} = \frac{13.1362}{\left[. \exp \frac{(1.6x\ 10^{-19} *3.1)}{82\ x\ 1.13\ x\ 1.38\ x\ 10^{-23}\ x\ 25}\right] - 1}$$

$$I_{rs} = \frac{13.1362}{[. \exp\ 15.5156\,] - 1}$$

$$I_{rs} = \frac{13.1362}{5.474,437.0146}$$

$$I_{rs} = 2.3996\ x\ 10^{-6}\ \text{A}$$

THE SATURATION CURRENT (IS) OF THE PHOTOVOLTAIC CELL

The saturation current of the solar module at cell temperature of 30, 40, 60 and 80 °C were obtained as follows:

$$I_S = I_{rs\ at\ ref\ temp} \left[\frac{T_c}{T_{ref}}\right]^3 \exp\left[\frac{q\ E_G\ \left(\frac{1}{T_{ref}} - \frac{1}{T_c}\right)}{KA}\right]$$

$$I_S = 2.3996\ x\ 10^{-6} \left[\frac{40}{25}\right]^3 \exp\left[\frac{1.6022 \times 10{-19}\ X\ 1.12\ eV\ \left(\frac{1}{25} - \frac{1}{40}\right)}{5.67\ x\ 10^{-8}\ X\ 1.13}\right]$$

$$I_S = 0.0000098288\ \exp[0.02762\ x\ 10^{-15}]$$

$$I_S = 0.0000098288\ A$$

THE OUTPUT CURRENT (I) OF THE PHOTOVOLTAIC MODULE

The output Currents (I) of the Photovoltaic module were determined using equation

$$I = I_{ph} - I_s \left[\exp\left(\frac{qV_{oc}}{AkT_c}\right) - 1\right]$$

$$I = 12.6862 - 0.0000098288 \left[\exp\left(\frac{1.6022 \times 10^{-19}\ x\ 3.1}{1.13\ X\ 1.38\ x\ 10^{-23}\ X\ 40}\right) - 1\right]$$

$$I = 12.6862 - 0.0000098288\ [\exp(9.7106\ x\ 10^4) - 1]$$

$$I = 12.6862 - 0.0000098288\ [16,490.493]$$

$$I = 12.6862 - 0.16208 = 12.5241\ A$$

T_{ref} = reference temperature

E_G = band gap energy of the semiconductor material used = 1.12 electron volt (eV)

I_{RS} = reverse saturation current at reference temperature of 25^0 C and solar radiance of 1000 W/m^2 = 2.3996 x 10^{-6} A

THE MAXIMUM POWER OF THE SOLAR MODULE AT VARYING TEMPERATURE

The Maximum power of the solar module at varying temperature were obtained and presented in figure 4.1 and table 4.1. We have taken 325 W silicon solar PV module as reference in this research work. The currently highest power polycrystalline silicon 60cell module is 325W.

Temperature coefficient of the maximum output power (Pmax) at STC is - 0.41%/°C.

With the solar module reaching 65°C, the power loss of this module was obtained as follows:

a. 65°C – 25°C = 40°C, which is the temperature difference between the module's Pmax at STC and the temperature of 65°C reached by the cells
b. 40°C x -0.41% = -16.4%, that means that the module loses 16.4% in power output when the cells reach 65°C
c. Power loss in the solar module = -16.4% x 3250W = 53.3 W.
d. The maximum power this module will operate at 65°C = 271.7 W.
e.

Table 4.1 Power loss in the Solar Photo Voltaic System with change in temperature

S/N	Temperature	T – 25	(T -25)x -0.41	Power loss (W)	Output power (W)
1	25	0	0	0	255
2	30	5	-2.05	5.227	249.773
3	40	15	-6.15	15.683	239317
4	60	35	-14.35	36.583	218.417
5	80	55	-22.55	57.503	197.498

The Subsystem Reverse Saturation Current under Varying Temperature Conditions and the Simulink Model

The subsystem reverse saturation current takes short circuit current, electric charge, open circuit voltage, ideality factor, temperature, open circuit voltage, number of series cells and Boltzmann's constant as input parameters

The reverse saturation current (Irs) is given by

$$I_{rs} = I_{SC} \big/ \left[.\exp \frac{(q*V_{oc})}{N_s AKT} - 1\right]$$
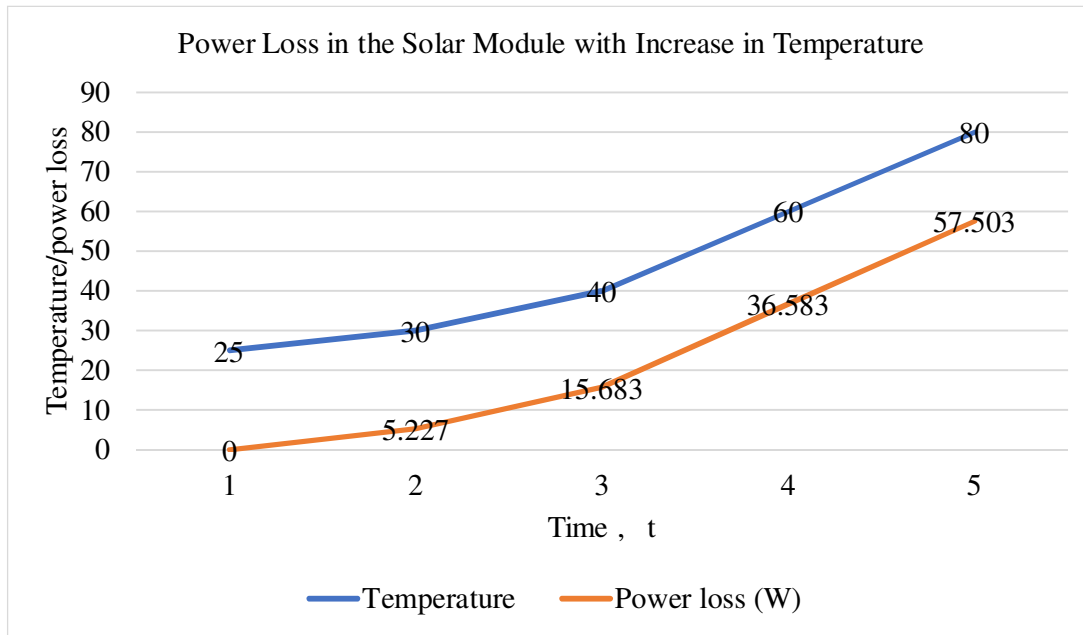
Figure 4.1: Power loss in the Solar Photo Voltaic System with change in temperature

Reverse saturation currents which vary with temperature were obtained and shown in table 4.2. The simulation results were presented in figure 4.2

Table 4.2: Irs for various temperature

S/N	Temperature (°C)	Reverse Saturation Current (A)
1	25	2.3996×10^{-6}
2	30	3.1800×10^{-5}
3	40	8.0725×10^{-4}
4	60	2.0200×10^{-2}
5	80	1.0379×10^{-1}
6	100	2.7731×10^{-1}

The Simulink model for reverse saturation current was implemented in Fig. 3.4.
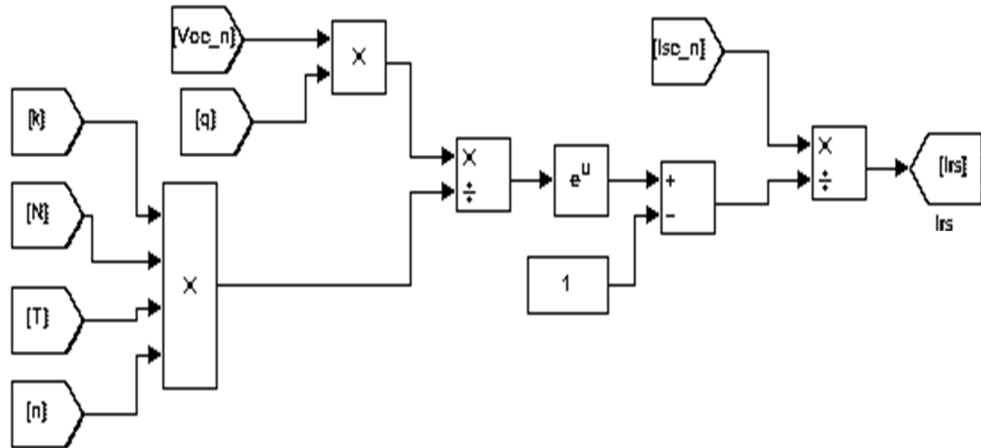

Fig.4.2. Subsystem of reverse saturation current

The subsystem module saturation current which varies with the cell temperature. These values were obtained and presented in table 4.3

$$I_S = I_{rs} \left[\frac{T}{T_r}\right]^3 \left[\exp\left(E_{g*} \frac{q\,(T-T_r)}{A*\,K.T.T_r}\right)\right]$$

Table 4.3 : Sauration current I_S for various temperatures

S/N	Temperature (°C)	Saturation Current (A)
1	25	2.3996×10^{-6}
2	30	4.1465×10^{-6}
3	40	9.8280×10^{-6}
4	60	3.3172×10^{-5}
5	80	7.8600×10^{-5}
6	100	1.5357×10^{-4}

The sub-system saturation current Simulink model was implemented and the result presented in figure 4.3
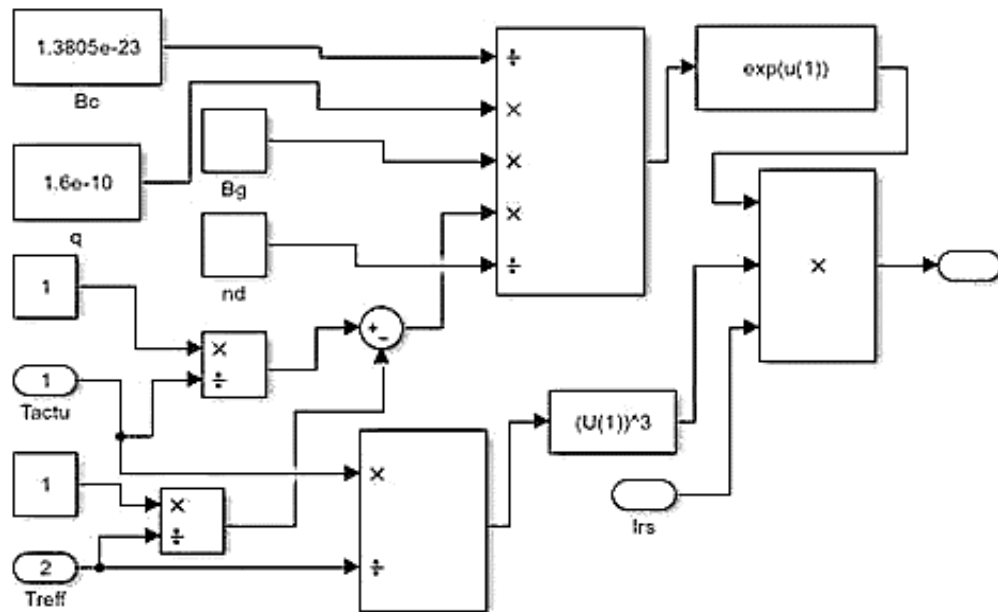
Figure 4.3: Subsystem of module saturation current.

The Subsystem Output Current Simulink Model

The subsystem output current I_{PV} mathematical model was simulated and the result was presented in figure 4.4

$$ 1 = N_P \left[I_{ph} - I_{rs} \ \langle \exp \left(\frac{q \ (V + I \ R_S)}{AKT \ N_S} - 1 \right) \rangle \right] $$
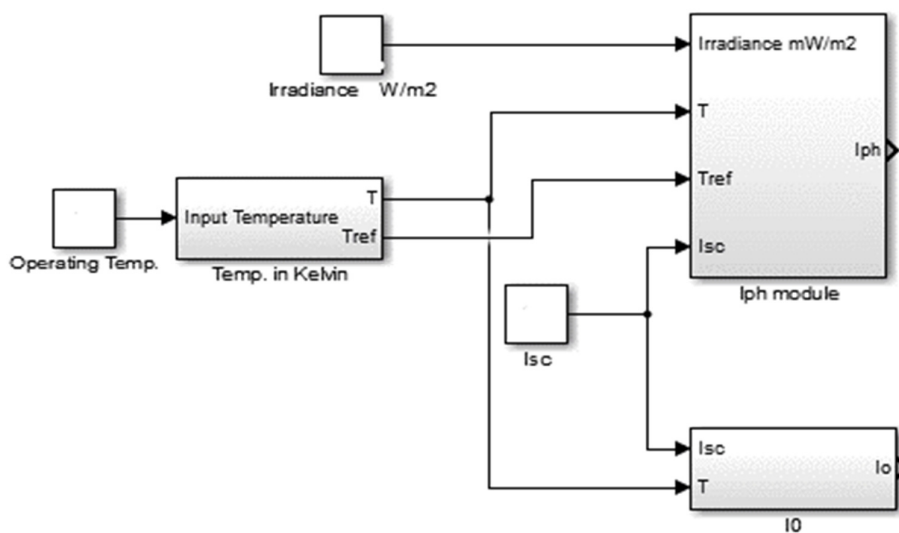
Figure 4.4: Subsystem of module output current.

The final model which produced the output current-voltage characteristics, and power-voltage characteristics of the solar system for varying irradiance and temperature are shown in figure 4.5
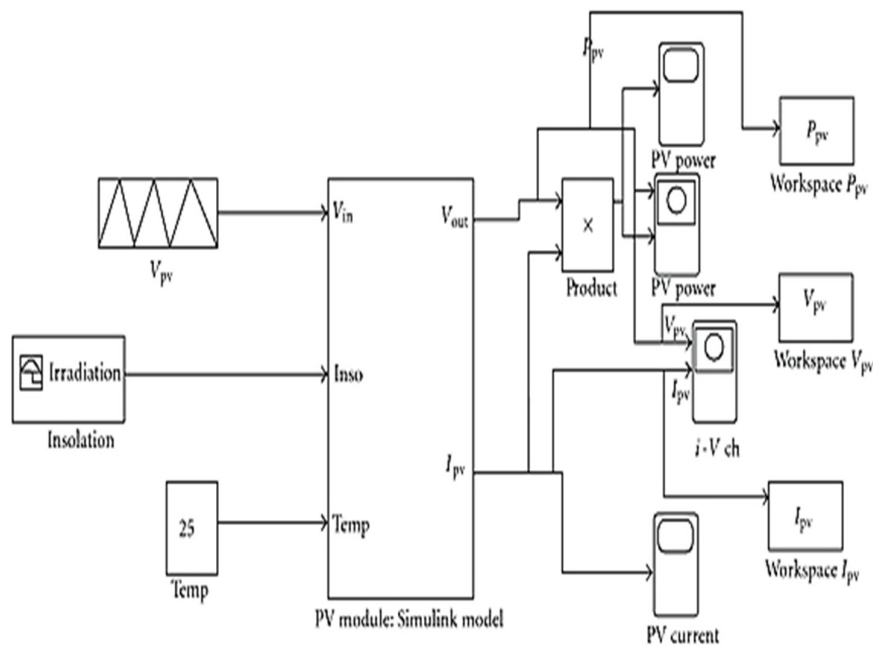

Fig. 4.5 : The final model produced the output voltage, current and power under varying irradiance and temperature

Optimum Power Point Tracking Techniques
Wind Turbine Generator Optimum Power Point Tracking Techniques
a. Tip Speed Ratio Control method

Power generated in a wind turbine generator was controlled using Tip Speed Ratio (TSR) control technique. The aim of this method of optimization process was to determine the optimum TSR. From the optimum TSR, the optimum angular rotor speed was obtained.

The TSR obtained was compared with the optimum value of TSR, which is already stored in the power system. The difference in the two values of TSR is fed to the controller which adjusted angular speed of the generator in order to ensure maximum power output as shown in the figure 4.6.
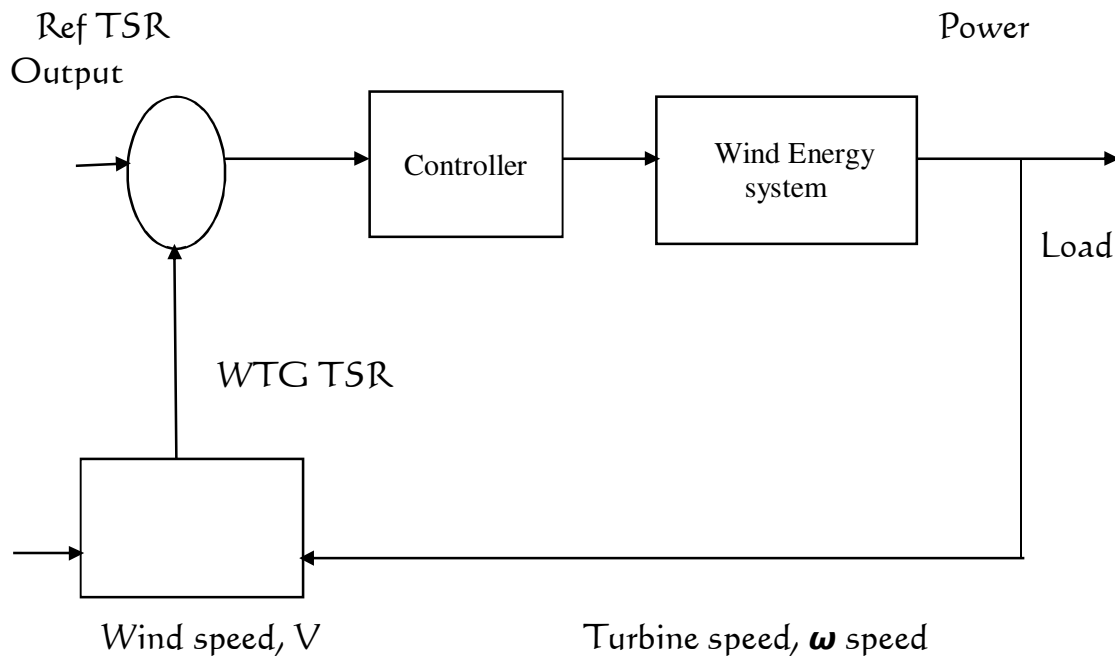
Ref TSR
Output

Power

```
                  ┌──────────────┐      ┌──────────────┐
  ──→ ( ) ───────→│  Controller  │─────→│ Wind Energy  │──────→
                  └──────────────┘      │   system     │
                                        └──────────────┘       Load
          WTG TSR

       ┌────────────┐
  ────→│            │←──────────────────────────────────────
       └────────────┘
```

WTG TSR

Wind speed, V   Turbine speed, ω speed

Figure 4.6: Working principle of TSR control techniques

Data Acquisition for the Wind Turbine Generator (WTG)

A 3.5 kW wind turbine generator proposed in Lagos State, Nigeria is taken as reference. The radius of the turbine blade is 1.12m. Average wind speed is 7m/s. Maximum Bertz coefficient of performance, C_p, is 0.5. Air density = 1.3 kg/m^3. Optimum Tip speed ratio , λ_{opt} is obtained when C_p is maximum. Optimum rotor speed, ω_{opt} is obtained during this Optimum Tip speed ratio as shown below.

$$\text{Optimum Tip Speed Ratio} = \lambda_{opt} = \frac{2P}{C_p \ \rho \ A \ V^3}$$

$$= \frac{2 \ x \ 3,500}{0.5 \ x \ 1.3 \ x \ 3.94 \ x \ 7^3} = 7.9688$$

The Optimum rotor speed, ω_{opt} was obtained for the proposed wind turbine generator as follows:

$$\text{Optimum Rotor Speed Ratio} = \omega_{opt} = \frac{\lambda_{opt} \ x \ V}{R}$$

$$= \frac{7.9688 \ x \ 7}{1.2} = 49.805 \text{ rad/sec}$$

The tip speed ratio, angular rotor speed and output power generated is presented in table 4.4a and b

Rω	0	33.6	36	44.8	50	56	60	67.2	75	78.4	100
Power Output (Watts)	0	1060	2100	2400	3100	3200	3100	2800	2200	1200	0

The tip speed ratio, angular rotor speed and output power generated is presented in table 4.4a

S/N	Radius of blade	ω	V	Rω	Tip Speed Ratio	Power Output
1	1.12	30	7	33.6	4.8	1,060
2	1.12	40	7	44.8	6.4	2,400
3	1.12	50	7	56.0	8.0	3,200
4	1.12	60	7	67.2	9.6	2,800
5	1.12	70	7	78.4	11.2	1,200

The tip speed ratio, angular rotor speed and output power generated is presented in table 4.4b

The characteristics of the rotor speed and the output power generated is presented in figure 4.7
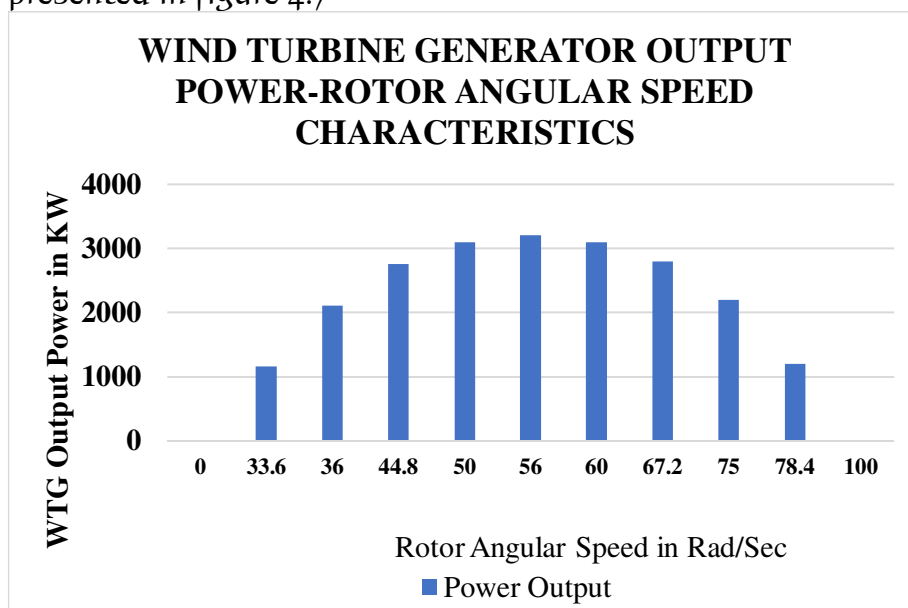

Figure 4.7: characteristics of the rotor speed and the output power generated from the wind turbine generator

Table 4.5 Shows the Monthly Output Power Produced by the Proposed Wind Turbine Generator in Watts

S/N	Months	Average Power Generated (Watts)	Average Wind Speed in m/s
1	January	1600	3.80
2	February	1800	4.22
3	March	2100	5.60
4	April	2200	5.81
5	May	2600	7.10
6	June	2100	5.60
7	July	1820	4.22
8	August	2140	5.61
9	September	3200	9.00
10	October	2860	8.40
11	November	1400	3.30
12	December	1650	4.00

Table 4.5: Monthly Output Power Produced by the Proposed Wind Turbine Generator in Watts

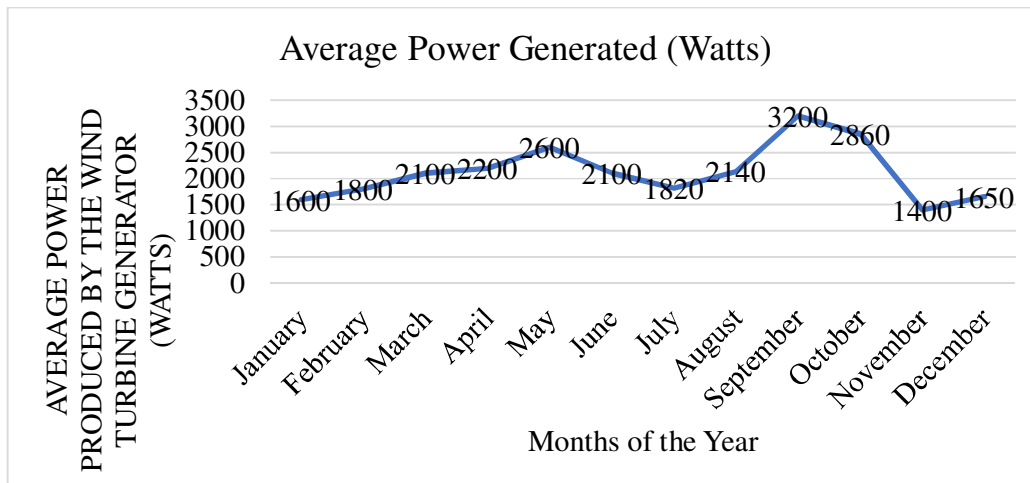Figure 4.8 shows the Monthly Output Power Produced by the Wind Turbine Generator in Watts

Figure 4.8: Monthly Output Power Produced by the Proposed Wind Turbine Generator in Watts

Figure 4.9 Shows the Monthly Average Wind Speed at the Reference Area in Meter/Second
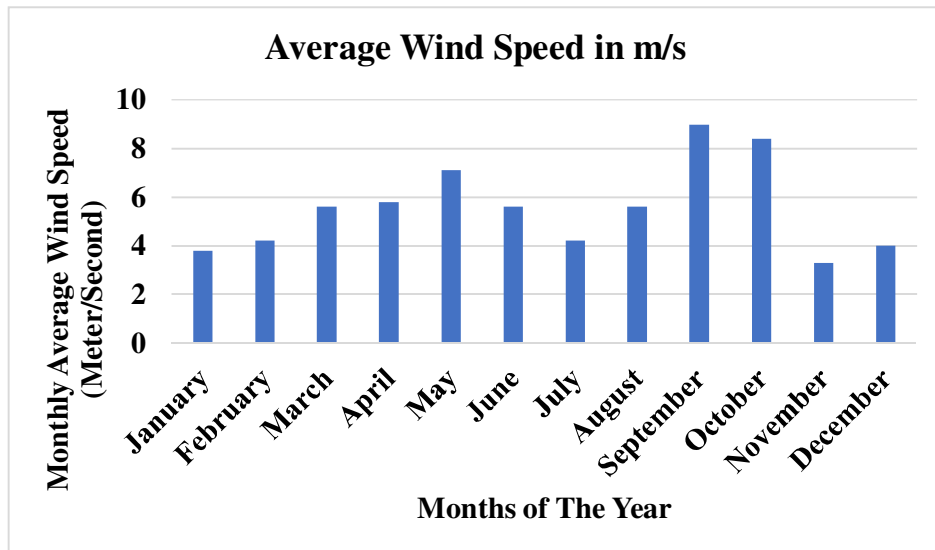

Figure 4.9: Monthly Average Wind Speed at the Reference Area in Meter/Second

Solar Energy Audit Data and Meteorological Data and Parameters of the Reference Site

Electrical Parameters of Photo-Voltaic cells were measured at specified temperature of 25 °C, solar irradiances 1000 W/m² and air mass 1.5 AM.

The number of solar panels at the reference area is 820. The solar module is 325 W each and the area of each module is $1.63 m^3$. The efficiency of the solar cell is 83.6 and the average annual solar radiation is 1367 kWhm^{-2}.

a. Energy consumption at the study area in watt hour = 1,865,500 Watt hour

This implies that the total energy to be supplied = 1,865,500 Wh

$$\text{Watt peak} = \frac{\text{Energy to be supplied}}{number\ of\ hours\ of\ sunlight}$$

$$\text{Watt peak} = \frac{1,865,500\ \text{Wh}}{7} = 266,500$$

$$\text{Number of 325 W panels} = \frac{\text{Watt peak}}{Wattage\ of\ a\ solar\ panel}$$

$$\text{Number of 325 W panels} = \frac{266,500}{325} = 820$$

b. System voltage = Voltage of a battery x number of batteries in series

$$= 12 \times 10 = 120 \text{ V}$$

c. Charge to be stored in the solar system = $\frac{Grand\ total\ energy \times Day(s)\ of\ autonomy}{System\ Voltage}$

Charge to be stored in the solar system $= \frac{1,865,500 \times 1}{120}$

$$= 15,545.833 \text{ Ampere hour (Ah)}$$

System Current $= \frac{Total\ power}{system\ voltage} = \frac{245,073.4}{120} = 510.57 \text{ A}$

d. 200 Ah batteries were proposed at the reference area

Number of batteries required = $\frac{Charge\ to\ be\ stored\ in\ the\ solar\ system}{rating\ of\ a\ battery\ in\ Ah \times depth\ of\ discharge}$

Hence, number of batteries required $= \frac{15,545.833}{200 \times 0.2} = 388.65 = 387$

b. Average solar insolation: 278–330 days of sun per year with daily average sunshine ranging from 7 hours during the rainy season to 9 hours in dry season

c. Solar radiation: 833.33 to 1341.67 kWh/m^2

Subsystem of photon generated current Iph for different values of irradiance and temperature were presented in table 4.6

Table 4.6 Subsystem of Photo Generated Current under varying temperature and irradiance

S/N	Temperature (°C)	Irradiance kW/m^2	Photo current(A)
1	25	1	13.1362
2	30	1	12.986
3	40	1	12.6862
4	60	1	12.0862
5	80	1	11.4862
6	100	1	10.8865

$$I_{ph} = I_{SCR} + k_1 [T - T_r]\frac{S}{100}$$
$$I_{ph} = I_{SCR} + k_1 [T - T_r]\lambda$$

The subsystem reverse saturation current takes short circuit current, temperature, open circuit voltage, number of series cells as input parameters
The reverse saturation current (Irs) is given b

$$I_{rs} \;=\; I_{SC} \;/\; \left[. \exp \; \frac{(q * V_{oc})}{N_s AKT} - 1 \right]$$

Reverse saturation currents varies with temperature were obtained and shown in table 4.7

Table 4.7: reverse saturation current Irs for various temperature

S/N	Temperature (°C)	Reverse Saturation Current (A)
1	25	2.3996×10^{-6}
2	30	3.1800×10^{-5}
3	40	8.0725×10^{-4}
4	60	2.0200×10^{-2}
5	80	1.0379×10^{-1}
6	100	2.7731×10^{-1}

4.15 The subsystem of module saturation current which varies with the cell temperature were obtained and presented in table 4.7

$$I_S \;=\; I_{rs} \left[\frac{T}{T_r} \right]^3 \left[\exp \; \left(\; E_{g*} \; \frac{q\,(T - T_r)}{A* \; K.T.T_r} \right) . \right]$$

Table 4.8 Sauration current I_S for various temperatures

S/N	Temperature (°C)	Saturation Current (A)
1	25	2.3996×10^{-6}
2	30	4.1465×10^{-6}
3	40	9.8280×10^{-6}
4	60	3.3172×10^{-5}
5	80	7.8600×10^{-5}
6	100	1.5357×10^{-4}

Simulation Results

The developed model was implemented for the sample module and the results were evaluated. The evaluation was done using the equations developed in the previous sections. The chosen module provides the output power of 255W and has 10 series cells. The IV and PV characteristics are modeled and simulated for the chosen module using the developed equations and models. Fig. 4.10 and fig. 4.11 show the IV and PV characteristics of module under varying irradiance at constant temperature respectively.

Table 4.9: I-V Curves with various Irradiance levels

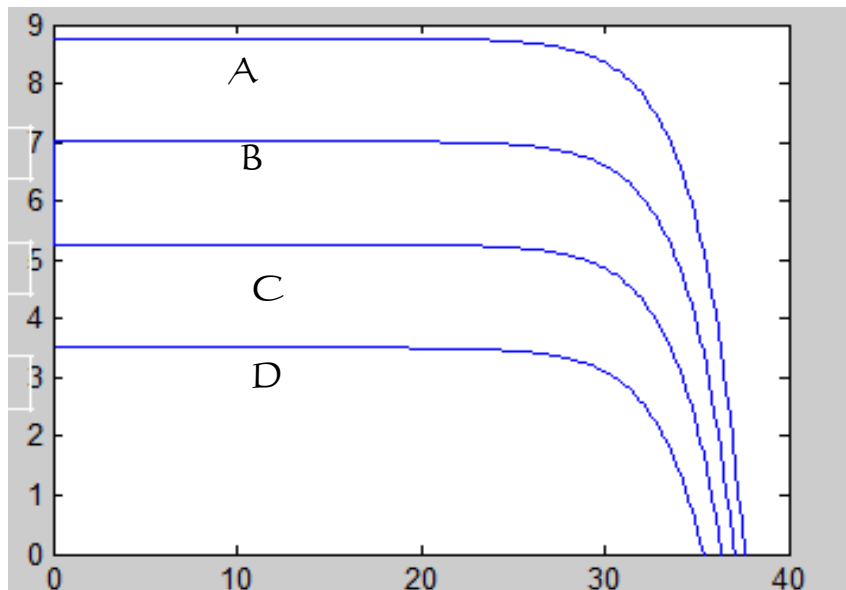| I - V Curves	Temperature in Kelvin 273 + T ref	Irradiance level in KW/m²
A	298	1
B	298	0.8
C	298	0.6
D	298	0.4

.

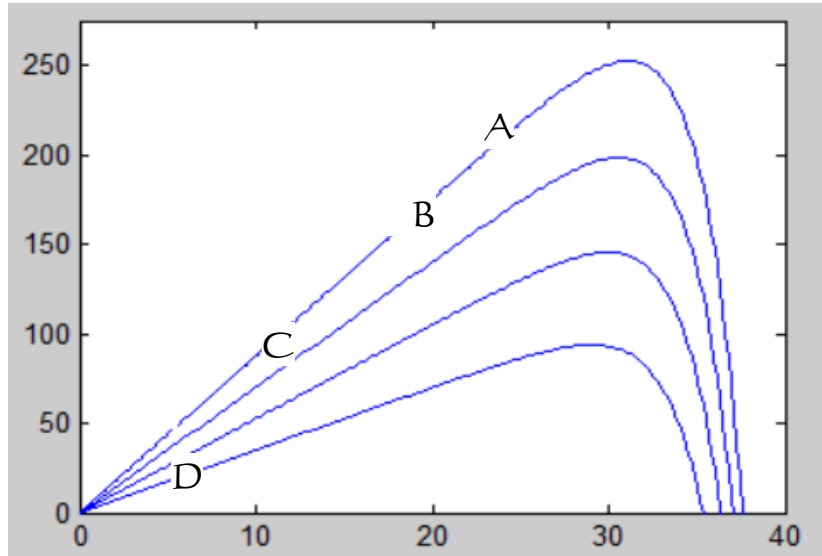Figure 4.10: IV characteristics under varying irradiance at constant temperature (298K)

Figure 4.11: PV characteristics under varying irradiance at constant temperature (298K)

Figure 4.10 and figure 4.11 show IV and the PV characteristics of module under varying temperature at constant irradiance respectively. From the characteristics, it is observed that there is an optimum operating point called maximum power point. This point changes with temperature and irradiance. This point increases with irradiance and decreases with temperature. Hence for the given photovoltaic system, it was possible to estimate the optimum power point.

Table 4.10: I-V Curves with various temperature levels

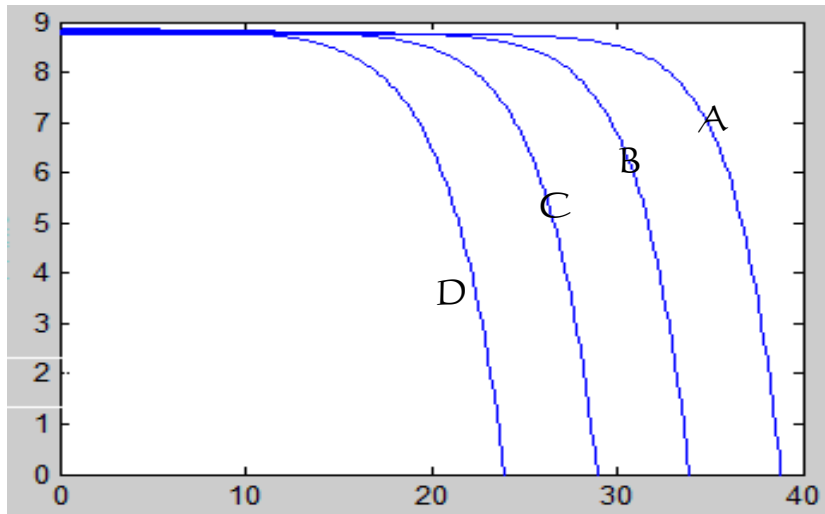| I - V Curves	Irradiance level in KW/m²	Temperature in Kelvin
A	1	298
B	1	318
C	1	338
D	1	358

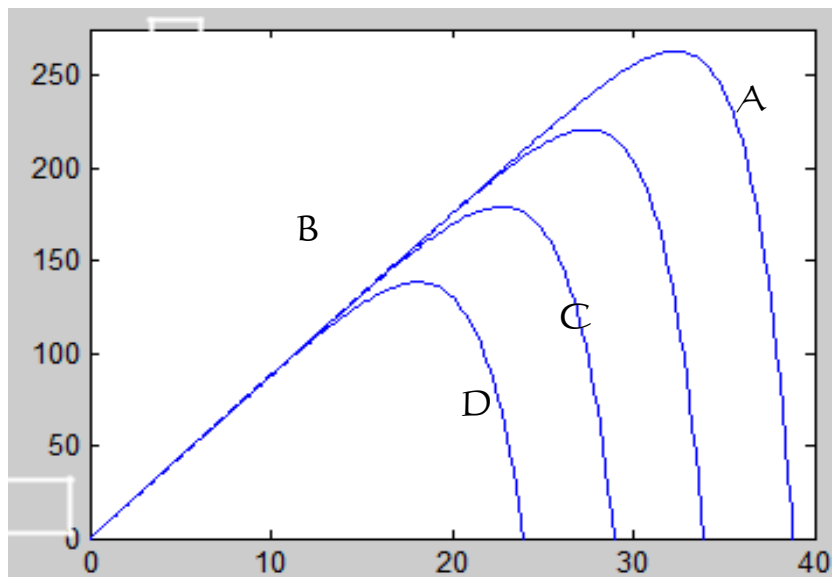Figure 4.12:   IV characteristics under varying temperature at constant irradiance (1KW/m²)

Fig. 4.13: PV characteristics under varying temperature at constant irradiance (1KW/m²)

In conclusion, a PV module was developed and modelled using Matlab/Simulink. From the model, it is understood that the output current is function of solar irradiance. The developed PV model is verified with the available module. The model could be used for analysis in the area of solar photovoltaic conversion system and MPPT technologies

Table 4.12 shows the Average monthly radiation of the reference area in kWh/meter square

S/N	Months	Average monthly radiation (kWh/meter square)
1	January	6.86
2	February	6.58
3	March	6.72
4	April	4.34
5	May	4.06
6	June	3.64
7	July	3.22
8	August	5.01
9	September	3.78
10	October	5.74
11	November	6.3
12	December	6.44

Table 4.12: Average monthly radiation of the reference area (kWh/meter square)

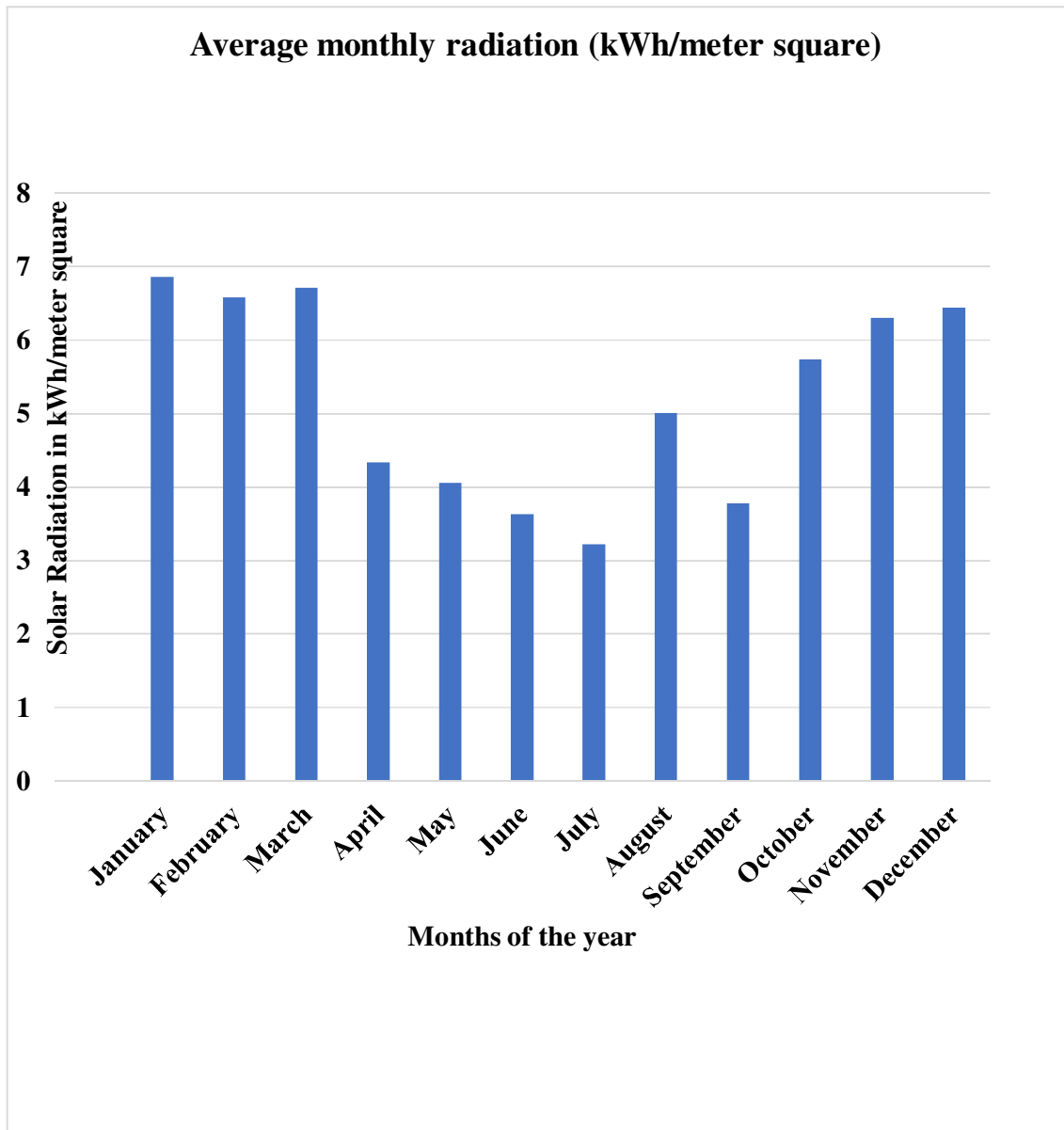Figure 4.11 shows the Average monthly radiation of the reference area in kWh/meter square

Average monthly radiation (kWh/meter square)

Figure 4.11: Average monthly radiation of the reference area in kWh/meter square

CONCLUSION
Solar radiation and power generation from the solar photo-voltaic system

Annual solar radiation at the reference area ranges between 3.22 kwh/m^3 to 6.86 kwh/m^3. The value of sun radiation in the study area is very high in the month of October – march i.e., during the dry season. The study revealed that the solar radiation during this period ranges between 5.74 kwh/m^3 to 6.86 kwh/m^3. Hence, the hybrid electric power system (heps) developed produced adequate and reliable solar electric power system between the six months as shown in tables 4.13 – 4.21 and figures 4.12, 4.14, 4.17 – 4.23. The reliability of the solar photo-voltaic power system during this period is 100%. The photo-current and reverse saturation current were presented in tables 4.5 and 4.6 respectively. However, solar radiation reduces during the months of april – september to the range of 3.22 kwh/m^3 to 4.34 kwh/m^3 as shown in figure 4.11. Consequently, the solar power generated during the rainy season reduces to 154w – 174w/module as presented in figure 4.16. Weather condition during this period reduced solar radiation and the electric power generated from the solar photo- voltaic system (spvs). As a result, the efficiency and relisability of the system reduces considerably. Therefore, the provision of other reliable power supply system increased the reliability of the system and ensured continuous supply of electrical energy to the consumers.

Solar Photo- Voltaic System (Spvs) and Hydro Electric Power System (Heps)

The proposed hydro-electric power plant developed in this research work provide adequate solution to the problem of low reliability of solar photo-voltaic system. The proposed power plant has generating capacity of 4,948.88 kw to 6,245.01 kw during the rainy season as sown in table 4.3 and 4.4. The discharge rate of Ikere River in iseyin community, oyo state, where the proposed hydro-electric power plant will be located ranges between 13.8 m^3/second in the month of February to 31.8 m^3/second in the month of September. This is presented in table 4.4 and figures 4.2, 4.3, 4.13, 4.20, 4.22 and 4.23. Output power developed during this period ranges between 4,948.88 kw and 6,245.01 kw. As a result, it was possible to supply adequate and continuous power supply to the consumers.

Solar photo-voltaic system simulation results

The simulation results presented in figures 4.4 – 4.7 show that solar power generated from the solar modules increases with increase in radiation and reduces as temperature rises above $25^0 c$. Table 4.10 represents variation of power loss in the photo-voltaic system with change in temperature. Figures 4.12 – 4.18 show the monthly electric power production from the hybrid solar photo-voltaic system, proposed hydro-electric power plant, proposed wind turbine generator and the diesel generator. the hybrid-electric power system produced adequate, reliable, stable power supply as shown in figures 4.19 - 4.23.

REFERENCE

Abubakar Sadiq Aliyu, Joseph O.Dada, Ibrahim KhalilAdam (2015), Current status and future prospects of renewable energy in Nigeria, Volume 48, August 2015,

Ali Keyhani, (2017) Design of smart power grid and renewable energy systems

An overview of solar power (PV systems) integration into electricity grids Mechanical Engineering Department, University of Botswana, Gaborone, Botswana

Austin, O. O., Lasisi, K. A., Adeniyi, A. J., & Alonge, O. (2020). Development of a Model for the Establishment of a Hydro Electric Power Generating Plant. *Journal La Multiapp*, *1*(3), 27-42. https://doi.org/10.37899/journallamultiapp.v1i3.207

Bekele, G. and Tadesse, G., "Feasibility Study of Small Hydro/PV/ Wind Hybrid System for Off-Grid Rural Electrification in Ethiopia," Applied Energy, Vol. 97, pp. 5-15, 2012.

Binayak Bhandari, Shiva Raj Poudel, Kyung-Tae Lee, and Sung-Hoon Ahn (2014), Mathematical Modeling of Hybrid Renewable Energy System: A Review on Small Hydro-Solar-Wind Power Generation

Design and Automation of a Hybrid System for Generating Electric Power, Mosiori, Cliff Ororiia and Maera, John, 2019

Design And Simulation of a PV System with Battery Storage Using Bidirectional DC-DC Converter Using Matlab Simulink, Mirza Mursalin Iqbal and Kafiul Islam, 2017

Ebele Stella. Chukwunonso Ekesiobi, 2017, Power infrastructure and electricity in Nigeria: Policy considerations for economic welfare

EliasM.Salilih and Yilma T.Birhane (2019), Modeling and Analysis of Photo-Voltaic Solar Panel under Constant Electric Load

EliasM.Salilih andYilmaT.Birhane (2019), Modeling and Analysis of Photo-Voltaic Solar Panel under Constant Electric Load

Fadaeenejad, M., Radzi, M. A. M., AbKadir, M. Z. A., and Hizam, H., "Assessment of Hybrid Renewable Power Sources for Rural Electrification in Malaysia," Renewable and Sustainable Energy Reviews, Vol. 30, pp. 299-305, 2014.

Hua, C. and Lin, J., "A Modified Tracking Algorithm for Maximum Power Tracking of Solar Array," Energy Conversion and Management, Vol. 45, No. 6, pp. 911-925, 2004.

Hybrid Renewable Energy Micro grid for a Residential Community: A Techno-Economic and Environmental Perspective in the Context of the SDG7, Nallapaneni Manoj Kumar et.al, 2020

Ibrahim Baba Kyari, Jamilu Ya'u Muhammad (2019), Hybrid Renewable Energy Systems for Electrification

Meenal Jain, Nilanshu Ramteke, (2013) Modeling and Simulation of Solar Photovoltaic module using Matlab / Simulink

Mustafa Engin mustafa (2012), Sizing and Simulation of PV-Wind Hybrid Power System
Nigeria Energy Situation, (energypedia.info, 2020).

Austin, O. O. (2021). Advanced Control and Development of Hydro and Diesel Generator Hybrid Power System Models for Renewable Energy Microgrids. *Journal La Multiapp*, *2*(3), 16-32. https://doi.org/10.37899/journallamultiapp.v2i3.383